Intelligent Block-Level Interference Exploitation Beamforming Design: An ADMM Approach

Yiran Wang, Yunsi Wen, Ang Li, Xiaoyan Hu, Christos Masouros
Department of Information and Communications Engineering, Xi'an Jiaotong University, Xi'an, Shaanxi 710049, China
Department of Electronic and Electrical Engineering, University College London, WC1E 7JE London, U.K.
{yiranwang, YunsiWen}@stu.xjtu.edu.cn, {ang.li.2020, xiaoyanhu}@xjtu.edu.cn, c.masouros@ucl.ac.uk

***Abstract*—We study constructive interference based block-level beamforming (CI-BLB) in the downlink of multi-user multiple-input single-output (MU-MISO) systems. CI-BLB achieves improved performance over the traditional CI-based symbol-level beamforming (CI-SLB) method, because of its more intelligent power allocation scheme over the considered block of symbol slots. In this paper, we design a low-complexity algorithm based on the alternating direction method of multipliers (ADMM) framework, which can efficiently solve QP problems. We analyze the convergence and complexity of the proposed algorithm. Numerical results validate the optimality of the proposed algorithm, and further show that the proposed algorithm offers a flexible performance-complexity tradeoff by limiting the maximum number of iterations, which motivates the use of CI-BLB in practical wireless systems.**

***Index Terms*—MIMO, constructive interference (CI), block-level beamforming (BLB), quadratic programming (QP) optimization, alternating direction method of multipliers (ADMM).**

I. Introduction

Beamforming has been widely studied in multiple-input multiple-output (MIMO) communication systems, which is able to support data transmission to multiple users simultaneously [1]. In the downlink, if the channel state information (CSI) is fully known to the base station, dirty paper coding (DPC) is proved to be capacity-achieving by pre-subtracting interference before transmission [2], but its prohibitive computational costs make it difficult to implement in practical systems. Therefore, low-complexity closed-form linear beamforming schemes, represented by zero-forcing (ZF) [3] and regularized ZF (RZF) [4], are proposed to reduce the computational complexity in signal processing. At the same time, optimization-based beamforming schemes are gaining more and more attention because they allow beamforming to better meet various communication constraints and requirements in different scenarios. One popular example is the downlink signal-to-interference-plus-noise ratio (SINR) balancing approach, which aims to achieve a desired SINR for each user under transmit power constraints [5]. Another popular form is to minimize the transmit power under the SINR constraint of each user [6]. [7] proves that the SINR balancing and the power minimization are dual problems to each other, where an effective iterative algorithm has been proposed by exploiting such duality to efficiently solve these two problems.

More recent research has shown that multi-user interference need not be completely eliminated in beamforming design. This is because interference can be utilized by interference exploitation beamforming techniques to benefit symbol detection, thus improving the error-rate performance of MIMO communication systems. In [8], the concept of 'constructive interference' (CI) is introduced, and CI-based beamforming has received increasing research attention. The concept of 'constructive region' is introduced in [9], which shows that as long as the interfered signals lie in the constructive region, the effect of interference is typo. In [10], the exploitation of CI was extended for the first time from PSK modulation to QAM modulation, where the CI effect can be exploited by the outer constellation points of a QAM constellation by employing the 'symbol-scaling' CI metric. Because of the significant advantages of CI, CI-based symbol-level beamforming (CI-SLB) has been applied to intelligent reflecting surface (IRS)-assisted communication [11], 1-bit precoding [12], radar-communication coexistence [13] and many other wireless communication scenarios.

It has to be mentioned that the utilization of CI in the above schemes is based on symbol-level beamforming, which brings significant computational burden to the signal processing unit and requires demanding real-time processing capability. To alleviate the computational costs, several studies attempt to reduce the complexity of the CI-SLB optimization problems, including derivations of the optimal beamforming structure of CI-SLB with efficient iterative algorithms [14], [15], sub-optimal solutions [16], [17], and deep learning-based methods [18], [19]. Despite the above attempts to reduce the computational costs of solving the CI-SLB optimization problem for each symbol slot, these approaches still require solving an optimization problem at the symbol level. In order to further motivate the realization of CI-based beamforming techniques in practical communication wireless systems, [20] proposed CI-based block-level beamforming (CI-BLB) for multi-user multiple-input single-output (MU-MISO) communication system for the first time. Based on Lagrange function and Karush-Kuhn-Tucker (KKT) condition, the closed-form expression of CI-BLB optimal beamforming matrix is derived. By further studying the corresponding duality problem, the original optimization problem is transformed into a quadratic programming (QP) optimization on simplex.

In this paper, we design a low-complexity solution for the

above CI-BLB based on the alternating direction method of multipliers (ADMM) framework, which can efficiently solve large-scale QP problems, thus appealing for application in solving CI-BLB problems. We analyze the convergence and complexity of the proposed algorithm. The proposed ADMM algorithm is able to offer satisfactory results within only dozens of iterations, while it is much faster than the traditional interior-point method (IPM) [21]. More importantly, the proposed ADMM algorithm is more time-efficient than *quadprog*, which motivates the use of the block-level CI beamforming in practice.

Notations: Herein, Lowercase, boldface lowercase and boldface uppercase letters denote scalars, vectors and matrices, respectively. $\mathbb{R}$ and $\mathbb{C}$ denote the set of real numbers and the set of complex numbers, respectively. Superscripts $^{\mathrm{T}}$ denotes the transpose. The operator $\|\cdot\|_2$ denotes the 2-norm of a vector. $\Re\{\cdot\}$ and $\Im\{\cdot\}$ extract the real and imaginary parts of the argument, respectively. We use $\Pi_{\mathbf{\Omega}}$ to represent the projection of the argument onto the set $\mathbf{\Omega}$. We define j as $\sqrt{-1}$ and $\mathbf{I}_N$ as the $N \times N$ identity matrix. Finally, $\mathbf{1}$ and $\mathbf{0}$ denote all-one vector and all-zero vector, respectively.

II. System Model and Preliminaries

A. System Model

We consider the generic multi-user multiple-input single-output (MU-MISO) downlink system, where a base station (BS) equipped with N_t antennas serves K single-antenna users simultaneously. For the transmission of a block of symbol slots, the data symbol vector in the n-th slot is denoted by $\mathbf{s}^n = [s_1^n, s_2^n, \cdots, s_K^n]^{\mathrm{T}} \in \mathbb{C}^K$, which is assumed to be drawn from a unit-norm $\mathcal{M}$-PSK constellation[1]. Accordingly, the received signal for user k in the n-th symbol slot can be expressed as

$$y_k^n = \mathbf{h}_k^{\mathrm{T}} \mathbf{W} \mathbf{s}^n + z_k^n, \tag{1}$$

where $\mathbf{h}_k \in \mathbb{C}^{N_t}$ is the channel between BS and user k, which is constant within the considered block, and $z_k^n \in \mathbb{C}$ is the additive noise of user k in the n-th symbol slot. $\mathbf{W} \in \mathbb{C}^{N_t \times K}$ is the beamforming matrix that applies to all $\mathbf{s}^n$ in the considered block. $n \in \{n | n \leq N\}$, where N is the length of the considered transmission block.

B. Symbol-Scaling CI Metric

CI can increase the useful signal power and greatly improve the performance of multi-user transmission. To illustrate the symbol-scaling CI meric introduced in [22], below we depict one quarter of an 8PSK constellation in Fig. 1 as an example. Without loss of generality, we assume that $\overrightarrow{OA}$ is the nominal constellation point for user k in the n-th slot, i.e.,

$$\overrightarrow{OA} = s_k^n. \tag{2}$$

$\overrightarrow{OB}$ represents the noiseless received signal with interference, where based on the geometry we obtain

$$\overrightarrow{OB} = \overrightarrow{OA} + \overrightarrow{AB} = \mathbf{h}_k^n \mathbf{W} \mathbf{s}^n, \tag{3}$$

[1]For the extension to QAM modulation, see [20].

where $\overrightarrow{AB}$ can be regarded as the interference from other user streams.

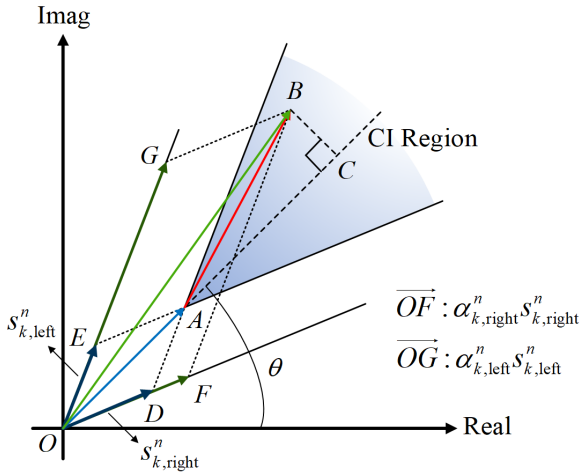

Fig. 1. Geometric diagram of the symbol-scaling CI metric for 8PSK.

Different from the common phase-rotation CI metric which uses phase relations, the symbol-scaling CI metric decomposes the signal along the decision boundaries and imposes scaling constraints on the decomposed components. In Fig. 1, $\overrightarrow{OA}$ is decomposed along the two decision boundaries for 8PSK modulation to obtain $\overrightarrow{OD}$ and $\overrightarrow{OE}$:

$$\overrightarrow{OA} = \overrightarrow{OD} + \overrightarrow{OE} = s_{k,\text{right}}^n + s_{k,\text{left}}^n. \tag{4}$$

Following a similar procedure, the received signal $\overrightarrow{OB}$ can also be decomposed along the two decision boundaries into

$$\overrightarrow{OB} = \overrightarrow{OF} + \overrightarrow{OG} = \alpha_{k,\text{right}}^n s_{k,\text{right}}^n + \alpha_{k,\text{left}}^n s_{k,\text{left}}^n. \tag{5}$$

By following the transformation in Section IV-A of [23], which we omit in this paper due to the limited space and also for brevity, we can construct a coefficient matrix $\mathbf{M}^n \in \mathbb{R}^{2K \times 2N_t}$ and obtain:

$$\boldsymbol{\alpha}_{\mathrm{E}}^n = \mathbf{M}^n \mathbf{W}_{\mathrm{E}} \mathbf{s}_{\mathrm{E}}^n, \tag{6}$$

where $\boldsymbol{\alpha}_{\mathrm{E}}^n \in \mathbb{R}^{2K}$, $\mathbf{W}_{\mathrm{E}} \in \mathbb{R}^{2N_t \times 2K}$ and $\mathbf{s}_{\mathrm{E}}^n \in \mathbb{R}^{2K}$ are defined as

$$\boldsymbol{\alpha}_{\mathrm{E}}^n = \left[\alpha_{1,\text{right}}^n, \cdots, \alpha_{K,\text{right}}^n, \alpha_{1,\text{left}}^n, \cdots, \alpha_{K,\text{left}}^n\right]^{\mathrm{T}}, \tag{7}$$

$$\mathbf{W}_{\mathrm{E}} = \begin{bmatrix} \Re(\mathbf{W}) & -\Im(\mathbf{W}) \\ \Im(\mathbf{W}) & \Re(\mathbf{W}) \end{bmatrix}, \ \mathbf{s}_{\mathrm{E}}^n = \left[\Re(\mathbf{s}^n)^{\mathrm{T}}, \Im(\mathbf{s}^n)^{\mathrm{T}}\right]^{\mathrm{T}}. \tag{8}$$

C. Problem Formulation for CI-BLB

Recalling Fig. 1, we can observe that the value of $\alpha_{k,\text{right}}^n$ or $\alpha_{k,\text{left}}^n$ represents the effect of inter-user interference, and a larger value of $\alpha_{k,\text{right}}^n$ or $\alpha_{k,\text{left}}^n$ means that the symbol is pushed further away from one of its decision boundary. Accordingly, we can then construct the CI-BLB optimization problem that maximizes the minimum value of the entry in

$\boldsymbol{\alpha}_{\mathrm{E}}^n$ for all the considered symbol slots within the block, given by

$$\begin{aligned}\mathcal{P}_0:\ &\max_{\mathbf{W}_{\mathrm{E}}}\ \min_{k,n}\ \alpha_k^n\\ &\text{s.t.}\ \ \boldsymbol{\alpha}_{\mathrm{E}}^n=\mathbf{M}^n\mathbf{W}_{\mathrm{E}}\mathbf{s}_{\mathrm{E}}^n,\ \forall n\le N,\\ &\quad\sum_{n=1}^{N}\|\mathbf{W}_{\mathrm{E}}\mathbf{s}_{\mathrm{E}}^n\|_2^2\le Np_0,\end{aligned}\tag{9}$$

where α_k^n represents the k-th entry in $\boldsymbol{\alpha}_{\mathrm{E}}^n$, and p_0 represents the transmit power budget per symbol slot.

Lemma 1: By formulating the dual problem, the original CI-BLB optimization problem $\mathcal{P}_0$ can be transformed into the following QP optimization:

$$\begin{aligned}\mathcal{P}_1:\ &\min_{\boldsymbol{\delta}_{\mathrm{E}}}\ \boldsymbol{\delta}_{\mathrm{E}}^{\mathrm{T}}\mathbf{U}\boldsymbol{\delta}_{\mathrm{E}}\\ &\text{s.t.}\ \ \mathbf{1}^{\mathrm{T}}\boldsymbol{\delta}_{\mathrm{E}}-1=0,\\ &\quad\delta_{\mathrm{E}}^m\ge 0,\ \forall m\in\{1,2,\cdots,2NK\},\end{aligned}\tag{10}$$

where the coefficient matrix $\mathbf{U}$ can be calculated in advance. By obtaining the optimal $\boldsymbol{\delta}_{\mathrm{E}}$ through $\mathcal{P}_1$, the optimal beamforming matrix $\mathbf{W}$ can be calculated.

Proof: See Section III of [20]. ∎

The analysis in [20] is conducted for the case of $N\ge K$, while the conclusions of the above lemma is also applicable for the case of $N<K$, which has been shown in [24]. Therefore, an efficient algorithm for $\mathcal{P}_1$ is the key to CI-BLB.

III. The Proposed ADMM Algorithm

A. The Proposed Algorithm

Proposition 1: $\mathcal{P}_1$ is equivalent to the following optimization problem:

$$\begin{aligned}\mathcal{P}_2:\ &\min_{\boldsymbol{\delta}_{\mathrm{E}}}\ \boldsymbol{\delta}_{\mathrm{E}}^{\mathrm{T}}\mathbf{U}\boldsymbol{\delta}_{\mathrm{E}}\\ &\text{s.t.}\ \ \mathbf{1}^{\mathrm{T}}\boldsymbol{\delta}_{\mathrm{E}}-1\ge 0,\\ &\quad\delta_{\mathrm{E}}^m\ge 0,\ \forall m\in\{1,2,\cdots,2NK\}.\end{aligned}\tag{11}$$

Proof: Assume that $\boldsymbol{\delta}_{\mathrm{E}}^*$ is an optimal solution to $\mathcal{P}_2$, we have

$$\mathbf{1}^{\mathrm{T}}\boldsymbol{\delta}_{\mathrm{E}}^*-1>0,\ \ (\delta_{\mathrm{E}}^*)^m\ge 0,\ \forall m\in\{1,2,\cdots,2NK\}.\tag{12}$$

Accordingly $\boldsymbol{\delta}_{\mathrm{E}}^{**}=\kappa\boldsymbol{\delta}_{\mathrm{E}}^*$, such that

$$\mathbf{1}^{\mathrm{T}}\boldsymbol{\delta}_{\mathrm{E}}^{**}-1=0,\ \ (\delta_{\mathrm{E}}^{**})^m\ge 0,\ \forall m\in\{1,2,\cdots,2NK\},\tag{13}$$

where $\kappa=\frac{1}{\mathbf{1}^{\mathrm{T}}\boldsymbol{\delta}_{\mathrm{E}}^*}\in(0,1)$. We then have

$$(\boldsymbol{\delta}_{\mathrm{E}}^{**})^{\mathrm{T}}\mathbf{U}\boldsymbol{\delta}_{\mathrm{E}}^{**}=\kappa^2(\boldsymbol{\delta}_{\mathrm{E}}^*)^{\mathrm{T}}\mathbf{U}\boldsymbol{\delta}_{\mathrm{E}}^*<(\boldsymbol{\delta}_{\mathrm{E}}^*)^{\mathrm{T}}\mathbf{U}\boldsymbol{\delta}_{\mathrm{E}}^*,\tag{14}$$

which contradicts the assumption that $\boldsymbol{\delta}_{\mathrm{E}}^*$ is an optimal solution to $\mathcal{P}_2$. Therefore, the optimal solution to $\mathcal{P}_2$ must satisfy $\mathbf{1}^{\mathrm{T}}\boldsymbol{\delta}_{\mathrm{E}}-1=0$, which means that the optimal solution to $\mathcal{P}_2$ is the optimal solution to $\mathcal{P}_1$, i.e., $\mathcal{P}_2$ is equivalent to $\mathcal{P}_1$. ∎

Based on the above proposition, to apply the ADMM framework, we introduce a new variable $\hat{\boldsymbol{\omega}}$ and define a set $\hat{\Omega}=\{\hat{\boldsymbol{\omega}}|\hat{\omega}_i\ge 0,\ \forall i\in\{1,2,\ldots,2NK+1\}\}$. $\mathcal{P}_2$ is then equivalent to:

$$\begin{aligned}\mathcal{P}_3:\ &\min_{\boldsymbol{\delta}_{\mathrm{E}}}\ \boldsymbol{\delta}_{\mathrm{E}}^{\mathrm{T}}\mathbf{U}\boldsymbol{\delta}_{\mathrm{E}}\\ &\text{s.t.}\ \ \begin{bmatrix}\mathbf{1}^{\mathrm{T}}\\ \mathbf{I}_{2NK\times 2NK}\end{bmatrix}\boldsymbol{\delta}_{\mathrm{E}}=\begin{bmatrix}1\\ \mathbf{0}\end{bmatrix}+\hat{\boldsymbol{\omega}},\\ &\quad\hat{\boldsymbol{\omega}}\in\hat{\Omega}.\end{aligned}\tag{15}$$

By defining an indicator function for $\hat{\boldsymbol{\omega}}$:

$$I_{\hat{\Omega}}(\hat{\boldsymbol{\omega}})=\begin{cases}0, & \text{if } \hat{\boldsymbol{\omega}}\in\hat{\Omega},\\ \infty, & \text{otherwise},\end{cases}\tag{16}$$

and

$$\boldsymbol{\Gamma}=\begin{bmatrix}\mathbf{1}^{\mathrm{T}}\\ \mathbf{I}_{2NK}\end{bmatrix}\in\mathbb{C}^{(2NK+1)\times(2NK)},\ \mathbf{c}=\begin{bmatrix}1\\ \mathbf{0}\end{bmatrix}\in\mathbb{C}^{(2NK+1)\times 1},\tag{17}$$

$\mathcal{P}_3$ can be written as

$$\begin{aligned}\mathcal{P}_4:\ &\min_{\boldsymbol{\delta}_{\mathrm{E}}}\ \boldsymbol{\delta}_{\mathrm{E}}^{\mathrm{T}}\mathbf{U}\boldsymbol{\delta}_{\mathrm{E}}+I_{\hat{\Omega}}(\hat{\boldsymbol{\omega}})\\ &\text{s.t.}\ \ \boldsymbol{\Gamma}\boldsymbol{\delta}_{\mathrm{E}}=\mathbf{c}+\hat{\boldsymbol{\omega}}.\end{aligned}\tag{18}$$

The corresponding augmented Lagrangian function for $\mathcal{P}_4$ is expressed as

$$\begin{aligned}&\hat{L}_\rho\left(\boldsymbol{\delta}_{\mathrm{E}},\hat{\boldsymbol{\omega}},\hat{\boldsymbol{\lambda}}\right)=\boldsymbol{\delta}_{\mathrm{E}}^{\mathrm{T}}\mathbf{U}\boldsymbol{\delta}_{\mathrm{E}}+I_{\hat{\Omega}}(\hat{\boldsymbol{\omega}})+\hat{\boldsymbol{\lambda}}^{\mathrm{T}}(-\boldsymbol{\Gamma}\boldsymbol{\delta}_{\mathrm{E}}+\mathbf{c}+\hat{\boldsymbol{\omega}})\\ &\quad+\frac{\rho}{2}\|-\boldsymbol{\Gamma}\boldsymbol{\delta}_{\mathrm{E}}+\mathbf{c}+\hat{\boldsymbol{\omega}}\|_2^2\\ &=\boldsymbol{\delta}_{\mathrm{E}}^{\mathrm{T}}\mathbf{U}\boldsymbol{\delta}_{\mathrm{E}}+I_{\hat{\Omega}}(\hat{\boldsymbol{\omega}})+\frac{\rho}{2}\left\|-\boldsymbol{\Gamma}\boldsymbol{\delta}_{\mathrm{E}}+\mathbf{c}+\hat{\boldsymbol{\omega}}+\frac{\hat{\boldsymbol{\lambda}}}{\rho}\right\|_2^2-\frac{\left\|\hat{\boldsymbol{\lambda}}\right\|_2^2}{2\rho},\end{aligned}\tag{19}$$

where $\boldsymbol{\lambda}\in\mathbb{C}^{(2NK+1)\times 1}$ is the dual vector and $\rho>0$ is the penalty parameter. The ADMM framework for the update of $\boldsymbol{\delta}_{\mathrm{E}}$, $\hat{\boldsymbol{\omega}}$, and $\hat{\boldsymbol{\lambda}}$ can be written as

$$\boldsymbol{\delta}_{\mathrm{E}}^{k+1}=\arg\min_{\boldsymbol{\delta}_{\mathrm{E}}}\ \hat{L}_\rho\left(\boldsymbol{\delta}_{\mathrm{E}},\hat{\boldsymbol{\omega}}^k,\hat{\boldsymbol{\lambda}}^k\right),\tag{20}$$

$$\hat{\boldsymbol{\omega}}^{k+1}=\arg\min_{\boldsymbol{\omega}}\ \hat{L}_\rho\left(\boldsymbol{\delta}_{\mathrm{E}}^{k+1},\hat{\boldsymbol{\omega}},\hat{\boldsymbol{\lambda}}^k\right),\tag{21}$$

$$\hat{\boldsymbol{\lambda}}^{k+1}=\hat{\boldsymbol{\lambda}}^k+\rho\left(-\boldsymbol{\Gamma}\boldsymbol{\delta}_{\mathrm{E}}^{k+1}+\mathbf{c}+\hat{\boldsymbol{\omega}}^{k+1}\right).\tag{22}$$

In the $\boldsymbol{\delta}_{\mathrm{E}}$-update, the optimization problem for $\boldsymbol{\delta}_{\mathrm{E}}$ can be written as

$$\min_{\boldsymbol{\delta}_{\mathrm{E}}}\ \ \boldsymbol{\delta}_{\mathrm{E}}^{\mathrm{T}}\mathbf{U}\boldsymbol{\delta}_{\mathrm{E}}+\frac{\rho}{2}\left\|-\boldsymbol{\Gamma}\boldsymbol{\delta}_{\mathrm{E}}+\mathbf{c}+\hat{\boldsymbol{\omega}}^k+\frac{\hat{\boldsymbol{\lambda}}^k}{\rho}\right\|_2^2.\tag{23}$$

For this unconstrained convex optimization problem, the optimal point $\boldsymbol{\delta}_{\mathrm{E}}^{t+1}$ should satisfy the condition that the gradient is zero, which leads to

$$\left(2\mathbf{U}+\rho\boldsymbol{\Gamma}^{\mathrm{T}}\boldsymbol{\Gamma}\right)\boldsymbol{\delta}_{\mathrm{E}}=\rho\boldsymbol{\Gamma}^{\mathrm{T}}\left(\mathbf{c}+\hat{\mathbf{w}}^k+\frac{\hat{\boldsymbol{\lambda}}^k}{\rho}\right).\tag{24}$$

Then we can get a closed-form solution for $\boldsymbol{\delta}_{\mathrm{E}}^{k+1}$

$$\boldsymbol{\delta}_{\mathrm{E}}^{k+1} = \left(2\mathbf{U} + \rho\boldsymbol{\Gamma}^{\mathrm{T}}\boldsymbol{\Gamma}\right)^{-1} \rho\boldsymbol{\Gamma}^{\mathrm{T}} \left(\mathbf{c} + \hat{\mathbf{w}}^{k} + \frac{\hat{\boldsymbol{\lambda}}^{k}}{\rho}\right). \quad (25)$$

In the $\boldsymbol{\omega}$-update, the optimization problem for $\boldsymbol{\omega}$ can be written as

$$\min_{\boldsymbol{\omega}} \; I_{\Omega}(\boldsymbol{\omega}) + \frac{\rho}{2} \left\| -\boldsymbol{\Gamma}\boldsymbol{\delta}_{\mathrm{E}}^{k+1} + \mathbf{c} + \hat{\boldsymbol{\omega}} + \frac{\hat{\boldsymbol{\lambda}}^{k}}{\rho} \right\|_2^2. \quad (26)$$

Then $\boldsymbol{\omega}$ needs to satisfy

$$-\rho \left(-\boldsymbol{\Gamma}\boldsymbol{\delta}_{\mathrm{E}}^{k+1} + \mathbf{c} + \hat{\boldsymbol{\omega}} + \frac{\hat{\boldsymbol{\lambda}}^{k}}{\rho} \right) \in \partial I_{\Omega}(\boldsymbol{\omega}), \quad (27)$$

and we can obtain

$$\hat{\boldsymbol{\omega}}^{k+1} = \mathrm{m}ax \left\{ \mathbf{0}, \boldsymbol{\Gamma}\boldsymbol{\delta}_{\mathrm{E}}^{k+1} - \mathbf{c} - \frac{\hat{\boldsymbol{\lambda}}^{k}}{\rho} \right\}. \quad (28)$$

The corresponding algorithm is summarized in Algorithm 1.

Algorithm 1 The proposed ADMM algorithm

1: **Input**: $\mathbf{s}$, $\mathbf{H}$
2: **Output**: $\boldsymbol{\delta}_{\mathrm{E}}$
3: **Initial**: $\boldsymbol{\delta}_{\mathrm{E}}^{1} = \hat{\boldsymbol{\omega}}^{1} = \hat{\boldsymbol{\lambda}}^{1} = \mathbf{0}$, $\mathbf{U}$, $\mathbf{c}$, $\boldsymbol{\Gamma}$, ρ, maximum number of iterations K_{max}.
4: **for** $k = 1, \cdots K_{max}$ **do**
5: Compute $\boldsymbol{\delta}_{\mathrm{E}}^{k+1}$ by (25);
6: Compute $\hat{\boldsymbol{\omega}}^{k+1}$ by (28);
7: Update $\hat{\boldsymbol{\lambda}}^{k+1}$ by (22);
8: **end for**
9: Output: $\boldsymbol{\delta}_{\mathrm{E}} = \boldsymbol{\delta}_{\mathrm{E}}^{K_{max}+1}$.

B. Convergence Analysis

First, the minimizer $\hat{\boldsymbol{\omega}}^{k+1}$ satisfies

$$\hat{L}_{\rho}\left(\boldsymbol{\delta}_{\mathrm{E}}^{k}, \hat{\boldsymbol{\omega}}^{k+1}, \hat{\boldsymbol{\lambda}}^{k}\right) \leq \hat{L}_{\rho}\left(\boldsymbol{\delta}_{\mathrm{E}}^{k}, \hat{\boldsymbol{\omega}}^{k}, \hat{\boldsymbol{\lambda}}^{k}\right). \quad (29)$$

It is easy to see that $\hat{L}_{\rho}\left(\boldsymbol{\delta}_{\mathrm{E}}, \hat{\boldsymbol{\omega}}^{k+1}, \hat{\boldsymbol{\lambda}}^{k}\right)$ is strongly convex with respect to $\boldsymbol{\delta}_{\mathrm{E}}$. Because of the property of strongly convex function:

$$\left(\partial_{\boldsymbol{\delta}_{\mathrm{E},1}} \hat{L}_{\rho}\left(\boldsymbol{\delta}_{\mathrm{E},1}, \hat{\boldsymbol{\omega}}^{k+1}, \hat{\boldsymbol{\lambda}}^{k}\right) - \partial_{\boldsymbol{\delta}_{\mathrm{E},2}} \hat{L}_{\rho}\left(\boldsymbol{\delta}_{\mathrm{E},2}, \hat{\boldsymbol{\omega}}^{k+1}, \hat{\boldsymbol{\lambda}}^{k}\right)\right)^{\mathrm{T}} \cdot \left(\boldsymbol{\delta}_{\mathrm{E},1} - \hat{\boldsymbol{\delta}}_{\mathrm{E},2}\right) \geq m \left\| \boldsymbol{\delta}_{\mathrm{E},1} - \hat{\boldsymbol{\delta}}_{\mathrm{E},2} \right\|_2^2, \quad (30)$$

where m is the strongly convex parameter of $\hat{L}_{\rho}\left(\boldsymbol{\delta}_{\mathrm{E}}, \hat{\boldsymbol{\omega}}^{k+1}, \hat{\boldsymbol{\lambda}}^{k}\right)$, we can obtain that

$$\begin{aligned} &\partial_{\boldsymbol{\delta}_{\mathrm{E},1}} \hat{L}_{\rho}\left(\boldsymbol{\delta}_{\mathrm{E},1}, \hat{\boldsymbol{\omega}}^{k+1}, \hat{\boldsymbol{\lambda}}^{k}\right) - \partial_{\boldsymbol{\delta}_{\mathrm{E},2}} \hat{L}_{\rho}\left(\boldsymbol{\delta}_{\mathrm{E},2}, \hat{\boldsymbol{\omega}}^{k+1}, \hat{\boldsymbol{\lambda}}^{k}\right) \\ &= \left(2\mathbf{U} + \rho\boldsymbol{\Gamma}^{\mathrm{T}}\boldsymbol{\Gamma}\right)\left(\boldsymbol{\delta}_{\mathrm{E},1} - \boldsymbol{\delta}_{\mathrm{E},2}\right). \end{aligned} \quad (31)$$

Since

$$\begin{aligned} \rho\boldsymbol{\Gamma}^{\mathrm{T}}\boldsymbol{\Gamma} &= \rho \begin{bmatrix} \mathbf{1} & \mathbf{I}_{2NK\times 2NK} \end{bmatrix} \begin{bmatrix} \mathbf{1}^{\mathrm{T}} \\ \mathbf{I}_{2NK\times 2NK} \end{bmatrix} \\ &= \rho\mathbf{1}\cdot\mathbf{1}^{\mathrm{T}} + \rho\mathbf{I}, \end{aligned} \quad (32)$$

where $\rho\mathbf{1}\cdot\mathbf{1}^{\mathrm{T}}$ is a semi-positive definite matrix and $\mathbf{U}$ is also a semi-positive definite matrix, we can obtain

$$\begin{aligned} &\left(\partial_{\boldsymbol{\delta}_{\mathrm{E},1}} \hat{L}_{\rho}\left(\boldsymbol{\delta}_{\mathrm{E},1}, \hat{\boldsymbol{\omega}}^{k+1}, \hat{\boldsymbol{\lambda}}^{k}\right) - \partial_{\boldsymbol{\delta}_{\mathrm{E},2}} \hat{L}_{\rho}\left(\boldsymbol{\delta}_{\mathrm{E},2}, \hat{\boldsymbol{\omega}}^{k+1}, \hat{\boldsymbol{\lambda}}^{k}\right)\right)^{\mathrm{T}} \\ &\cdot \left(\boldsymbol{\delta}_{\mathrm{E},1} - \boldsymbol{\delta}_{\mathrm{E},2}\right) \\ &= \left(\boldsymbol{\delta}_{\mathrm{E},1} - \boldsymbol{\delta}_{\mathrm{E},2}\right)^{\mathrm{T}} \left(2\mathbf{U} + \rho\boldsymbol{\Gamma}^{\mathrm{T}}\boldsymbol{\Gamma}\right)\left(\boldsymbol{\delta}_{\mathrm{E},1} - \boldsymbol{\delta}_{\mathrm{E},2}\right) \\ &= \left(\boldsymbol{\delta}_{\mathrm{E},1} - \boldsymbol{\delta}_{\mathrm{E},2}\right)^{\mathrm{T}} \left(2\mathbf{U} + \rho\mathbf{1}\cdot\mathbf{1}^{\mathrm{T}} + \rho\mathbf{I}\right)\left(\boldsymbol{\delta}_{\mathrm{E},1} - \boldsymbol{\delta}_{\mathrm{E},2}\right) \\ &\geq \rho \left\| \boldsymbol{\delta}_{\mathrm{E},1} - \boldsymbol{\delta}_{\mathrm{E},2} \right\|_2^2. \end{aligned} \quad (33)$$

Thus, $m = \rho$ and $\hat{L}_{\rho}\left(\boldsymbol{\delta}_{\mathrm{E}}, \hat{\boldsymbol{\omega}}^{k+1}, \hat{\boldsymbol{\lambda}}^{k}\right)$ is ρ-strongly convex with respect to $\boldsymbol{\delta}_{\mathrm{E}}$.

Similarly, by definition of strongly convex function:

$$\begin{aligned} &\hat{L}_{\rho}\left(\boldsymbol{\delta}_{\mathrm{E},1}, \hat{\boldsymbol{\omega}}^{k+1}, \hat{\boldsymbol{\lambda}}^{k}\right) \geq \hat{L}_{\rho}\left(\boldsymbol{\delta}_{\mathrm{E},2}, \hat{\boldsymbol{\omega}}^{k+1}, \hat{\boldsymbol{\lambda}}^{k}\right) \\ &+ \left(\partial_{\boldsymbol{\delta}_{\mathrm{E},2}} \hat{L}_{\rho}\left(\boldsymbol{\delta}_{\mathrm{E},2}, \hat{\boldsymbol{\omega}}^{k+1}, \hat{\boldsymbol{\lambda}}^{k}\right)\right)^{\mathrm{T}} \left(\boldsymbol{\delta}_{\mathrm{E},1} - \boldsymbol{\delta}_{\mathrm{E},2}\right) \\ &+ \frac{\rho}{2} \left\| \boldsymbol{\delta}_{\mathrm{E},1} - \boldsymbol{\delta}_{\mathrm{E},2} \right\|_2^2. \end{aligned} \quad (34)$$

The minimizer $\boldsymbol{\delta}_{\mathrm{E}}^{k+1}$ satisfies

$$\partial_{\boldsymbol{\delta}_{\mathrm{E}}^{k+1}} \hat{L}_{\rho}\left(\boldsymbol{\delta}_{\mathrm{E}}^{k+1}, \hat{\boldsymbol{\omega}}^{k+1}, \hat{\boldsymbol{\lambda}}^{k}\right) = \mathbf{0}. \quad (35)$$

Thus, for any $\boldsymbol{\delta}_{\mathrm{E}}^{k}$, the minimizer $\boldsymbol{\delta}_{\mathrm{E}}^{k+1}$ also satisfies

$$\begin{aligned} &\hat{L}_{\rho}\left(\boldsymbol{\delta}_{\mathrm{E}}^{k+1}, \hat{\boldsymbol{\omega}}^{k+1}, \hat{\boldsymbol{\lambda}}^{k}\right) \\ &\leq \hat{L}_{\rho}\left(\boldsymbol{\delta}_{\mathrm{E}}^{k}, \hat{\boldsymbol{\omega}}^{k+1}, \hat{\boldsymbol{\lambda}}^{k}\right) - \frac{\rho}{2} \left\| \boldsymbol{\delta}_{\mathrm{E}}^{k+1} - \boldsymbol{\delta}_{\mathrm{E}}^{k} \right\|_2^2. \end{aligned} \quad (36)$$

Moreover, from the definition of $\hat{L}_{\rho}$ and with the use of (22), we have

$$\begin{aligned} &\hat{L}_{\rho}\left(\boldsymbol{\delta}_{\mathrm{E}}^{k+1}, \hat{\boldsymbol{\omega}}^{k+1}, \hat{\boldsymbol{\lambda}}^{k+1}\right) - \hat{L}_{\rho}\left(\boldsymbol{\delta}_{\mathrm{E}}^{k+1}, \hat{\boldsymbol{\omega}}^{k+1}, \hat{\boldsymbol{\lambda}}^{k}\right) \\ &= \frac{1}{\rho} \left\| \hat{\boldsymbol{\lambda}}^{k+1} - \hat{\boldsymbol{\lambda}}^{k} \right\|_2^2. \end{aligned} \quad (37)$$

Then, summing (29), (36) and (37) yields

$$\begin{aligned} &\hat{L}_{\rho}\left(\boldsymbol{\delta}_{\mathrm{E}}^{k+1}, \hat{\boldsymbol{\omega}}^{k+1}, \hat{\boldsymbol{\lambda}}^{k+1}\right) - \hat{L}_{\rho}\left(\boldsymbol{\delta}_{\mathrm{E}}^{k}, \hat{\boldsymbol{\omega}}^{k}, \hat{\boldsymbol{\lambda}}^{k}\right) \\ &\leq \frac{1}{\rho} \left\| \hat{\boldsymbol{\lambda}}^{k+1} - \hat{\boldsymbol{\lambda}}^{k} \right\|_2^2 - \frac{\rho}{2} \left\| \boldsymbol{\delta}_{\mathrm{E}}^{k+1} - \boldsymbol{\delta}_{\mathrm{E}}^{k} \right\|_2^2. \end{aligned} \quad (38)$$

From (24), the minimizer $\boldsymbol{\delta}_{\mathrm{E}}^{k+1}$ satisfies

$$\left(2\mathbf{U} + \rho\boldsymbol{\Gamma}^{\mathrm{T}}\boldsymbol{\Gamma}\right)\boldsymbol{\delta}_{\mathrm{E}}^{k+1} - \rho\boldsymbol{\Gamma}^{\mathrm{T}} \left(\mathbf{c} + \hat{\mathbf{w}}^{k+1} + \frac{\hat{\boldsymbol{\lambda}}^{k}}{\rho}\right) = \mathbf{0}. \quad (39)$$

Substituting (22) into (39) we have

$$2\mathbf{U}\boldsymbol{\delta}_{\mathrm{E}}^{k+1} - \boldsymbol{\Gamma}^{\mathrm{T}}\hat{\boldsymbol{\lambda}}^{k+1} = \mathbf{0}, \quad (40)$$

which means

$$\begin{aligned} &\left\| \hat{\boldsymbol{\lambda}}^{k+1} - \hat{\boldsymbol{\lambda}}^{k} \right\|_2^2 \\ &= \left\| 2\mathbf{U}\left(\boldsymbol{\delta}_{\mathrm{E}}^{k+1} - \boldsymbol{\delta}_{\mathrm{E}}^{k}\right) \right\|_2^2 \\ &\leq 4\varphi^2 \left\| \boldsymbol{\delta}_{\mathrm{E}}^{k+1} - \boldsymbol{\delta}_{\mathrm{E}}^{k} \right\|_2^2, \end{aligned} \quad (41)$$

where $\varphi = \mathrm{eig}_{\max}(\mathbf{U})$.

Substituting (41) into (38) further results in

$$\hat{L}_\rho\left(\boldsymbol{\delta}_{\mathrm{E}}^{k+1}, \hat{\boldsymbol{\omega}}^{k+1}, \hat{\boldsymbol{\lambda}}^{k+1}\right) \leq \hat{L}_\rho\left(\boldsymbol{\delta}_{\mathrm{E}}^{k}, \hat{\boldsymbol{\omega}}^{k}, \hat{\boldsymbol{\lambda}}^{k}\right) - \left(\frac{\rho}{2} - \frac{4\varphi^2}{\rho}\right)\left\|\boldsymbol{\delta}_{\mathrm{E}}^{k+1} - \boldsymbol{\delta}_{\mathrm{E}}^{k}\right\|_2^2, \quad (42)$$

which means if the condition

$$\rho > 2\sqrt{2}\varphi \quad (43)$$

holds, $\hat{L}_\rho$ is monotonously decreasing in the iteration procedure. This completes the proof for convergence.

C. Complexity Analysis

We analyze the computational complexity of the proposed algorithm in terms of the number of real multiplication operations.

Considering the special structure of $\boldsymbol{\Gamma}$ shown in (17) and $\boldsymbol{\Gamma}^{\mathrm{T}}\boldsymbol{\Gamma}$ shown in (32), the computational complexity can be greatly reduced. In line 5 of Algorithm 1, the computation of $\left(2\mathbf{U} + \boldsymbol{\Gamma}^{\mathrm{T}}\boldsymbol{\Gamma}\right)^{-1}$ requires $\frac{1}{3}(2NK)^3$ real multiplications, which involve the cost of computing the Cholesky factorization. The computation of the matrix product of $\left(2\mathbf{U} + \boldsymbol{\Gamma}^{\mathrm{T}}\boldsymbol{\Gamma}\right)^{-1}\boldsymbol{\Gamma}^{\mathrm{T}}\left(\mathbf{c} + \hat{\mathbf{w}}^k + \hat{\boldsymbol{\lambda}}^k\right)$ requires $2NK(2NK+1)$ real multiplications. The total cost of $\boldsymbol{\delta}_{\mathrm{E}}$-update is $\left(\frac{1}{3}(2NK)^3 + 2NK(2NK+1)\right)$ real multiplications. The cost of projection $\hat{\boldsymbol{\omega}}$-update in line 6 is negligible. And the $\hat{\boldsymbol{\lambda}}$-update in line 7 does not require any real multiplication. Therefore, Algorithm 1 requires $\left(\frac{1}{3}(2NK)^3 + 2NK(2NK+1)\right)$ real multiplications when $k = 1$.

Given that $\left(2\mathbf{U} + \boldsymbol{\Gamma}^{\mathrm{T}}\boldsymbol{\Gamma}\right)^{-1}$ does not change in each iteration, we can cache the result to perform the subsequent iterations efficiently. Accordingly, Algorithm 1 requires $2NK(2NK+1)$ real multiplications for each iteration when $k \geq 2$. The total number of real multiplications for Algorithm 1 is $\left[\frac{1}{3}(2NK)^3 + T \cdot 2NK(2NK+1)\right]$, where T denotes the number of iterations.

IV. Simulation Results

We assume standard Rayleigh fading channel, random complex Gaussian distributed noise. The signal transmitting power is $p_0 = 1$, and the SNR is defined as $\frac{1}{\sigma^2}$, where σ^2 is the noise power. The execution time results are obtained from a Windows 11 Desktop with i9-10900 and 16GB RAM.

For clarity, the following abbreviations are used throughout this section:

1) ZF: Traditional ZF beamforming with block-level power normalization;
2) RZF: Traditional ZF beamforming with block-level power normalization;
3) CI-SLB-QP: Traditional CI-SLB solved by *quadprog* in *matlab*, $\mathcal{P}_8$ in [14];
4) CI-BLB-IPM: CI-BLB solved by IPM, $\mathcal{P}_1$;
5) CI-BLB-QP: CI-BLB solved by *quadprog* in *matlab*, $\mathcal{P}_1$;
6) CI-BLB-ADMM(K_{max}): CI-BLB solved by the proposed ADMM algorithm based on $\mathcal{P}_2$ with the maximum number of iterations K_{max}.

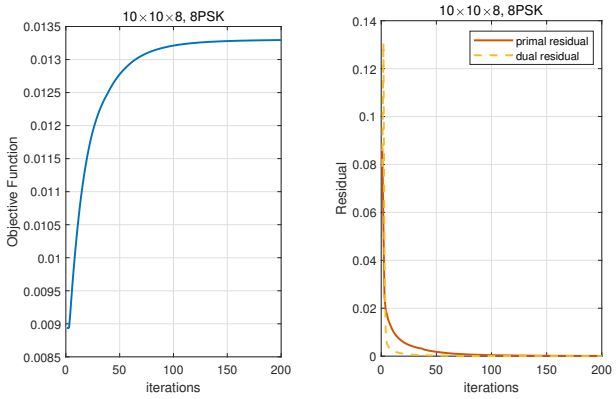

Fig. 2. Convergence behavior of the proposed ADMM algorithm, $N_t = K = 10$, $N = 8$, 8PSK. (a) Objective value. (b) Primal residual and dual residual.

For general ADMM iterative convergence, it is necessary to analyze the objective value, primal residual and dual residual [25]. We take $\rho = 1$ and obtained Fig. 2. In Fig. 2, (a) and (b) show the change of objective value and the change of residual with the number of iterations, respectively.

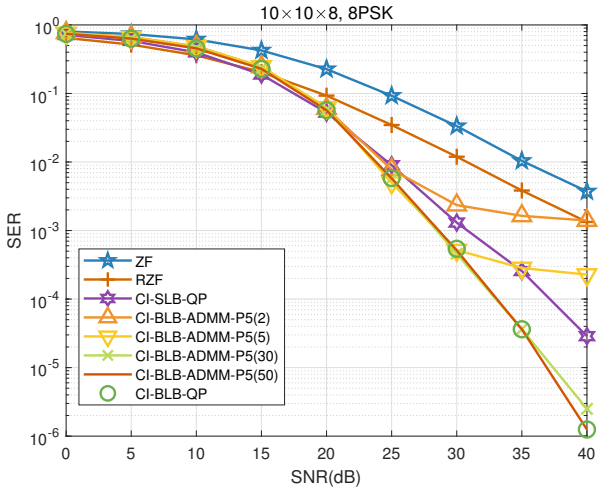

Fig. 3. SER performance of different schemes, $N_t = K = 10$, 8PSK.

Fig. 3 depicts the SER of the proposed CI-BLB scheme when 8PSK modulation is employed in a 10×10 MU-MISO system, where the length of the block is $N = 8$. As can be observed, both CI-based beamforming achieve an improved performance over ZF beamforming. When the length of the block is $N = 8$, we observe that CI-BLB offers noticeable performance gains over traditional CI-SLB, owing to the relaxed power constraint over the entire block. We observe

that a flexible trade-off between SER performance and computational complexity can be achieved by selecting different maximum iterations for the proposed ADMM algorithm.

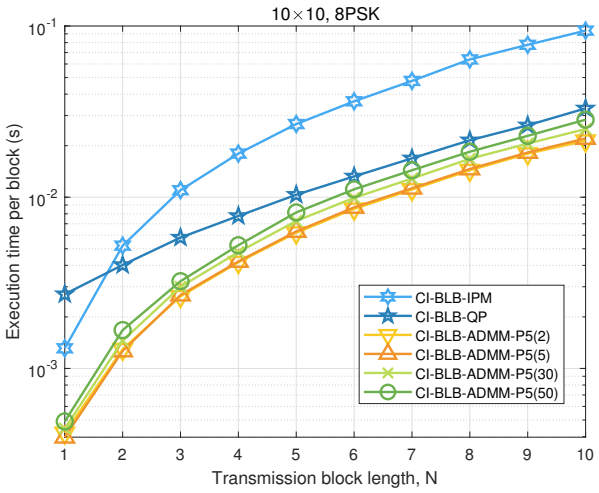

Fig. 4. SER performance of different schemes, $N_t = K = 10$, 8PSK, 30dB.

In Fig. 4 we compare the execution time required for each scheme as an indication to show the potential complexity benefits of the proposed ADMM algorithm. It is observed that the proposed ADMM algorithm is much faster than traditional IPM. More importantly, our proposed ADMM algorithm is more time-efficient than *quadprog*, which motivates the use of the block-level CI beamforming in practice.

V. Conclusion

In this paper, we propose a new ADMM algorithm for CI-BLB in a MU-MISO system. All subproblems have simple closed-form solutions, and convergence of the iterative ADMM algorithm has been proved. The proposed algorithm is shown to achieve the optimal performance with reduced computational costs, leading to favourable performance-complexity tradeoffs, which enables the use of block-level CI beamforming in practical wireless systems.

References

[1] L. Zheng and D. Tse, "Diversity and Multiplexing: A Fundamental Tradeoff in Multiple-Antenna Channels," *IEEE Transactions on Information Theory*, vol. 49, no. 5, pp. 1073–1096, 2003.

[2] M. Costa, "Writing on Dirty Paper," *IEEE Transactions on Information Theory*, vol. 29, no. 3, pp. 439–441, 1983.

[3] T. Haustein, C. von Helmolt, E. Jorswieck, V. Jungnickel, and V. Pohl, "Performance of MIMO Systems with Channel Inversion," in *Vehicular Technology Conference. IEEE 55th Vehicular Technology Conference. VTC Spring 2002 (Cat. No.02CH37367)*, vol. 1, 2002, pp. 35–39 vol.1.

[4] C. Peel, B. Hochwald, and A. Swindlehurst, "A Vector-Perturbation Technique for Near-Capacity Multiantenna Multiuser Communication-Part I: Channel Inversion and Regularization," *IEEE Transactions on Communications*, vol. 53, no. 1, pp. 195–202, 2005.

[5] A. Wiesel, Y. Eldar, and S. Shamai, "Linear Precoding via Conic Optimization for Fixed MIMO Receivers," *IEEE Transactions on Signal Processing*, vol. 54, no. 1, pp. 161–176, 2006.

[6] M. Bengtsson and B. Ottersten, "Optimal and Suboptimal Transmit Beamforming," *Handbook of aAntennas in Wireless Communications*, 2001.

[7] M. Schubert and H. Boche, "Solution of the Multiuser Downlink Beamforming Problem with Individual SINR Constraints," *IEEE Transactions on Vehicular Technology*, vol. 53, no. 1, pp. 18–28, 2004.

[8] C. Masouros, T. Ratnarajah, M. Sellathurai, C. B. Papadias, and A. K. Shukla, "Known Interference in the Cellular Downlink: A Performance Limiting Factor or A Source of Green Signal Power?" *IEEE Communications Magazine*, vol. 51, no. 10, pp. 162–171, 2013.

[9] C. Masouros and G. Zheng, "Exploiting Known Interference as Green Signal Power for Downlink Beamforming Optimization," *IEEE Transactions on Signal Processing*, vol. 63, no. 14, pp. 3628–3640, 2015.

[10] M. Alodeh, S. Chatzinotas, and B. Ottersten, "Symbol-Level Multiuser MISO Precoding for Multi-Level Adaptive Modulation," *IEEE Transactions on Wireless Communications*, vol. 16, no. 8, pp. 5511–5524, 2017.

[11] R. Liu, M. Li, Q. Liu, and A. L. Swindlehurst, "Joint Symbol-Level Precoding and Reflecting Designs for IRS-Enhanced MU-MISO Systems," *IEEE Transactions on Wireless Communications*, vol. 20, no. 2, pp. 798–811, 2021.

[12] A. Li, F. Liu, C. Masouros, Y. Li, and B. Vucetic, "Interference Exploitation 1-Bit Massive MIMO Precoding: A Partial Branch-and-Bound Solution With Near-Optimal Performance," *IEEE Transactions on Wireless Communications*, vol. 19, no. 5, pp. 3474–3489, 2020.

[13] F. Liu, C. Masouros, A. Li, T. Ratnarajah, and J. Zhou, "MIMO Radar and Cellular Coexistence: A Power-Efficient Approach Enabled by Interference Exploitation," *IEEE Transactions on Signal Processing*, vol. 66, no. 14, pp. 3681–3695, 2018.

[14] A. Li and C. Masouros, "Interference Exploitation Precoding Made Practical: Optimal Closed-Form Solutions for PSK Modulations," *IEEE Transactions on Wireless Communications*, vol. 17, no. 11, pp. 7661–7676, 2018.

[15] A. Li, C. Masouros, B. Vucetic, Y. Li, and A. L. Swindlehurst, "Interference Exploitation Precoding for Multi-Level Modulations: Closed-Form Solutions," *IEEE Transactions on Communications*, vol. 69, no. 1, pp. 291–308, 2021.

[16] A. Haqiqatnejad, F. Kayhan, and B. Ottersten, "Power Minimizer Symbol-Level Precoding: A Closed-Form Suboptimal Solution," *IEEE Signal Processing Letters*, vol. 25, no. 11, pp. 1730–1734, 2018.

[17] Y. Liu and W.-K. Ma, "Symbol-Level Precoding is Symbol-Perturbed zf When Energy Efficiency is Sought," in *2018 IEEE International Conference on Acoustics, Speech and Signal Processing (ICASSP)*, 2018, pp. 3869–3873.

[18] A. Mohammad, C. Masouros, and Y. Andreopoulos, "An Unsupervised Learning-Based Approach for Symbol-Level-Precoding," in *2021 IEEE Global Communications Conference (GLOBECOM)*, 2021, pp. 1–6.

[19] A. Mohammad, C. Masouros, and Y. Andreopoulos, "An Unsupervised Deep Unfolding Framework for Robust Symbol-Level Precoding," *IEEE Open Journal of the Communications Society*, vol. 4, pp. 1075–1090, 2023.

[20] A. Li, C. Shen, X. Liao, C. Masouros, and A. L. Swindlehurst, "Practical Interference Exploitation Precoding without Symbol-by-Symbol Optimization: A Block-Level Approach," *IEEE Transactions on Wireless Communications*, vol. 22, no. 6, pp. 3982–3996, 2023.

[21] S. Boyd and L. Vandenberghe, *Convex Optimization*. Cambridge University Press, 2004.

[22] A. Li, D. Spano, J. Krivochiza, S. Domouchtsidis, C. G. Tsinos, C. Masouros, S. Chatzinotas, Y. Li, B. Vucetic, and B. Ottersten, "A Tutorial on Interference Exploitation via Symbol-Level Precoding: Overview, State-of-the-Art and Future Directions," *IEEE Communications Surveys & Tutorials*, vol. 22, no. 2, pp. 796–839, 2020.

[23] A. Li, C. Masouros, F. Liu, and A. L. Swindlehurst, "Massive MIMO 1-Bit DAC Transmission: A Low-Complexity Symbol Scaling Approach," *IEEE Transactions on Wireless Communications*, vol. 17, no. 11, pp. 7559–7575, 2018.

[24] Y. Wang, Y. Wen, A. Li, X. Hu, and C. Masouros, "Block-Level Interference Exploitation Precoding for MU-MISO: An ADMM Approach," *arXiv e-prints*, p. arXiv:2308.12749, Aug. 2023.

[25] S. Boyd, N. Parikh, E. Chu, B. Peleato, and J. Eckstein, *Distributed Optimization and Statistical Learning via the Alternating Direction Method of Multipliers*, 2011.